PHYSICAL REVIEW C VOLUME 22, NUMBER 5 NOVEMBER 1980

$E2$ giant resonances and an $M1$ component in the photofission of ^{236}U

J. D. T. Arruda-Neto,* S. B. Herdade, B. L. Berman,† and I. C. Nascimento
Instituto de Fisica, Universidade de São Paulo, São Paulo, Brazil
(Received 15 October 1979)

Electrofission and photofission yields and electrofission-fragment angular distributions for ^{236}U have been measured with fission-track detectors for incident electron energies from 5.5 to 33.0 MeV. Analysis of these data with the use of virtual-photon spectra calculated in distorted-wave Born approximation, combined with the known photofission cross section, results in the simultaneous determination for this nucleus of (a) a giant isoscalar $E2$ resonance located at 10.8 ± 0.4 MeV, having a width of 6 ± 1 MeV, and exhausting $\sim 70\%$ of the isoscalar energy-weighted sum rule, and (b) a small $M1$ component located at 5.8 ± 0.2 MeV whose strength is $< 2\%$ of that of the giant isoscalar $E2$ resonance. No evidence is seen for a giant isovector $E2$ resonance between 22 and 30 MeV.

[NUCLEAR REACTIONS ^{236}U(e,f); measured fission-fragment yields and angular distributions, 5.5 to 33.0 MeV; deduced GQR characteristics.]

I. INTRODUCTION

The giant electric dipole resonance (GDR), discovered more than 30 years ago and located at energies ranging from 73 to $81A^{-1/3}$ MeV, is one of the best known and most familiar characteristics of the nuclear spectrum; it has been studied through all of the photonuclear reactions, and for most of the elements of the periodic table.[1]

The "new" giant resonances, i.e., those having multipolarities other than $E1$, have been studied only recently, mainly by means of the inelastic scattering of electrons and hadrons.[2-4] More recently still, combined results from electrofission and photofission measurements have been used as well to study the new giant resonances for very heavy nuclei.[5,6] Among these new resonances, the most thoroughly studied is the giant isoscalar electric quadrupole resonance (GQR), located just below the GDR at excitation energies from 60 to $65A^{-1/3}$ MeV, and predicted theoretically by Bohr and Mottelson.[7]

An isovector GQR also was predicted theoretically[7] and detected near $130A^{-1/3}$ MeV, but the experimental results are neither as abundant nor as convincing as for the isoscalar GQR.[2]

For the case of a giant magnetic dipole resonance, the experimental evidence is still controversial, but it is believed that such a resonance might be located in the energy range from 30 to $45A^{-1/3}$ MeV.[3,4] However, the experimental evidence supporting the existence of such a resonance for heavy nuclei is not compelling.

Substantial uncertainties are associated with the methods heretofore utilized most extensively for the study of the new giant resonances, namely, inelastic electron, proton, deuteron, and alpha-particle scattering, for at least two reasons. First, there are difficulties which stem from the subtraction of the large continuous backgrounds that appear under the observed peaks; and second, the analysis of inelastic-scattering data requires the use of phenomenological models, so that these methods never can give a model-independent determination of the multipolarity of the transition.

The electro-excitation of nuclear reactions has proved to be a sensitive tool for the study of $E2$ and $M1$ excitations involved in photonuclear reactions. This sensitivity results from the fact that the intensities of the $E2$ and $M1$ virtual-photon spectra calculated in the distorted-wave Born approximation (DWBA) are considerably larger than that for the $E1$ spectrum,[8] whereas for real photons the spectral intensities are the same for all multipoles. For example, Fig. 1 shows the $E1$, $E2$, and $M1$ virtual-photon spectra for an uranium nucleus ($Z = 92$) and for an incident electron kinetic energy of 9.5 MeV.[8] Although for real photons the $E2$ and $M1$ cross sections are typically much smaller than the $E1$ cross section, it is clear from Fig. 1 that the use of electro-excitation measurements facilitates greatly the observation and delineation of the $E2$ and $M1$ parts of the photon absorption cross section. The accuracy of the $E1$ virtual-photon spectra calculated in DWBA has been demonstrated by Nacimento *et al.*[9] The uncertainty in the $E2$ spectra is no larger than 20%.[10]

Even though one is faced with the disadvantage of dealing with integrated yields (as a function of excitation energy) in the analysis of electro-excitation data with the virtual-photon formalism, the advantages of this technique, compared with single-armed inelastic-scattering experiments, are considerable. These are (a) the absence of any significant background to be subtracted from the yields;

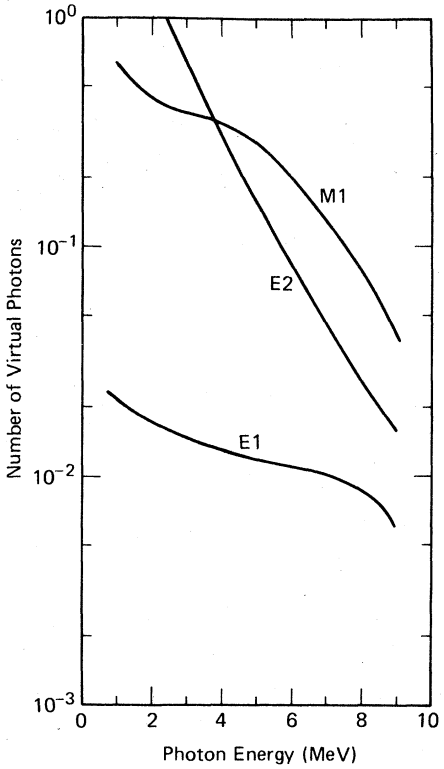

FIG. 1. $E1$, $E2$, and $M1$ virtual-photon spectra calculated in DWBA for electrons having energy $E_0 = 9.5$ MeV incident upon uranium ($Z = 92$) nuclei (from Ref. 8).

(b) the independence from nuclear models; (c) the insensitivity to $E0$ transitions (relative to $E2$ transitions) because of the overwhelming dominance of very-low-momentum-transfer events; and (d) at low energies, the ability to distinguish $E2$ from $E0$ transitions by means of the analysis of the electrofission-fragment angular distributions.

For the actinide nuclei, experimental information on the new resonances have been very sparse. Only ^{238}U has been the subject of reasonably intense study, through the analysis of the electrofission cross section,[11,12] fission induced by electrons and positrons,[13] and inelastic scattering of protons.[14] All these studies had the purpose of estimating the relative contributions of the $E1$ and $E2$ multipolarities, and the results obtained are not conclusive in the sense that they do not include the parameters of the detected resonances. Very recently, however, coincidence studies of the $(\alpha, \alpha' f)$ (Ref. 15) and (^{6}Li, ^{6}Li$'f$) (Ref. 16) reactions have been reported, with strongly conflicting and controversial results regarding the absence[15] or presence[16] of the fission channel as a major decay mode of the GQR. These results for ^{238}U are discussed at length in Ref. 17; the results for ^{236}U are the subject of the present paper. It suffices here to note that part of the controversy owes its origin to the equating of the fission probability with the strength of the GQR. The reader is referred to Ref. 17 for details.

The new technique used here, and described in Ref. 5, for obtaining the $E2$ and $M1$ components in the photofission channel requires the following experimental data: (a) the electrofission cross section, (b) the electrofission-fragment angular distributions near the fission barrier, and (c) accurate photofission cross sections measured with real photons. This last information is now available for several actinide nuclei from recent measurements performed by a joint Los Alamos–Livermore collaboration at Lawrence Livermore Laboratory.[18] The final result is obtained by the unfolding of an integral yield curve; in order to obtain reliable results it is necessary (a) to have as many data points as possible to delineate the yield curve (this is a well-known characteristic of unfolding techniques) and (b) to have data points as low in energy as possible to avoid a dubious extrapolation to the reaction threshold. Therefore, the (e,f) yield data must be obtained from energies below the fission barrier at ~6 MeV in small steps (≤ 0.25 MeV), and extended up to energies well above the resonances under study (~30 MeV); such measurements therefore require the use of an electron accelerator that operates reasonably well from ~5 MeV.

Although the photofission of ^{236}U has been studied elsewhere,[18–20] no information on the giant multipolar resonances other than the GDR has been obtained. No previous electrofission measurements for this isotope have been reported. The present study of ^{236}U was motivated mainly by the necessity of a systematic study of the new resonances in the actinide region and by the desirability of the study of a nucleus similar to ^{238}U (although its fissionability is quite different), not only in order to increase the data base for the very heavy nuclei, but also as an important test of the analysis techniques employed. Preliminary results for ^{236}U (Ref. 6) indicate the presence of the isoscalar GQR in the photofission channel having properties very similar to those for ^{238}U, as well as the presence of a third component, different from $E1$ and $E2$, near 6 MeV, whose separation and identification is accomplished in this work by means of a detailed analysis of the fission-fragment angular distributions. In addition, the data have been extended in energy up to 33 MeV in order to establish limits for the strength of the isovector giant $E2$ resonance predicted to be located near 22 MeV.

II. EXPERIMENTAL DETAILS

Many of the experimental features of the present measurements have been described previously.[5,11,21] Only the more important of these features and the details particular to the present experiment are described here.

The electrofission yields and fragment angular distributions reported here were obtained by irradiating thin targets of ^{236}U with the electron beam from the University of São Paulo Linear Accelerator, in steps of 0.5 MeV from 6.0 to 15.5 MeV and of 1.0 MeV from 15.5 to 26.5 MeV and from 26.0 to 33.0 MeV. The fission fragments were detected with mica-foil track detectors (whose efficiency is 100%) located at twelve different angles between 10° and 100° for energies up to 11.5 MeV and at seven angles for the higher energies. A 2π counting geometry (a ^{236}U target and a detector placed against it) also was used to measure electrofission yields at 5.5 MeV and from 5.75 to 11.75 MeV in steps of 0.5 MeV, and bremsstrahlung-induced fission yields from 9 to 19 MeV in steps of 2 MeV.

The target samples were of UO_2, enriched to 89.38% ^{236}U, vapor plated onto 5-μm thick titanium backing foils. The diameter of the UO_2 samples is 4.45 cm, and their thicknesses are 218 $\mu g/cm^2$. The vapor plating was performed at 2800 °C while the flat backing foils were simultaneously revolving about the central axis of the plating boat and rotating about their own axes, in order to smooth out density irregularities. The mass of ^{236}U was obtained indirectly to $\pm 2\%$ by simultaneously making an identical deposit on a weighable substrate and alpha counting to obtain a specific activity for the material used. The uniformity of the central 3.8-cm spot was verified to $\pm 2\%$ by alpha counting of 1.25-mm diameter spots across the target surface. The principal isotopic contaminant was ^{235}U (9.20%), whose effect on the fission yields and angular distributions was accounted for with the use of independent electron- and bremsstrahlung-induced fission measurements with pure $^{235}UO_2$ foils performed under identical experimental conditions. Spurious fission events caused by room-returned (thermalized) neutrons interacting with the ^{235}U contaminant were found to be of negligible importance by means of an experimental check in which a ^{235}U foil adjacent to the reaction chamber was exposed both with and without a cadmium-foil wrapping. The target foils were aligned at 45° to the electron-beam direction.

The size of the electron-beam spot at the target position was measured to be approximately 1 cm in diameter at 6 MeV, and smaller at higher energies. Particular care was given to the monitoring of the absolute beam intensity, with a short-necked Faraday cup coupled directly to the reaction chamber, close to the target position. The beam size at the entrance to the Faraday cup also was measured with a target foil in place and was found to be ~3 cm in diameter at 6 MeV, comfortably smaller than the 7-cm-diam aperture, even at low energies. Beam-off runs of 1–2 h duration showed that leakage currents in the Faraday cup were negligible, even when an external voltage (up to several hundred volts) was applied. No nonlinear response was likely at the low beam currents ($\lesssim 1$ μA) used for the experimental runs. The energy of the electron beam was monitored with a rotating-coil gaussmeter, and was calibrated, by means of an activation technique with reference to the photoneutron thresholds of ^{63}Cu (10.84 MeV) and ^{12}C (18.72 MeV), to be accurate to $\pm 1\%$ (~60 keV at 6 MeV) throughout the energy range studied.

The bremsstrahlung runs were performed with a copper radiator whose thickness is 0.076 radiation length (0.962 g/cm^2). Contamination (of the order of 20%) of the photofission yields with electrofission events was accounted for by means of the method developed by Barber.[22]

Other backgrounds, resulting from neutrons at the target location and from bremsstrahlung photons contaminating the electron beam, were shown to be negligible,[21] as were the effects of target thickness on the angular distributions or on the absolute cross sections.[21]

Other details of the accelerator, beam-transport system, shielding walls, reaction chamber, monitoring devices, and detection techniques and procedures can be found in Refs. 11 and 21.

III. DATA ANALYSIS

The number of fission tracks observed at each angle during an experimental run at a given energy was typically between 2000 and 3000 (sometimes reaching 5000), so that the total number of fission events (per energy) ranged from 20 000 to 30 000.

The electrofission differential cross section $d\sigma_e/d\Omega$, is obtained from

$$\frac{d\sigma_e(\theta)}{d\Omega}=\frac{1}{2N_t\phi}\left[\frac{N(\theta)}{\Delta\Omega}\right], \tag{1}$$

where N_t is the number of target nuclei, ϕ the number of electrons per cm^2, $N(\theta)$ the number of fission tracks in a mica detector located at angle θ (as explained in Sec. II) and whose area S defines a solid angle $\Delta\Omega = S/R^2$, where R is the radius of the reaction chamber, and hence the distance from sample to detector.

An angular distribution having the form

$$\frac{N(\theta)}{\Delta\Omega}=A+B\sin^2\theta+C\sin^2 2\theta \tag{2}$$

has been assumed.[21] The coefficients A, B, and C were obtained by the least-squares fitting of Eq. (2) to the experimental data.

The total electrofission cross section is given by

$$\sigma_e=\int\frac{d\sigma_e(\theta)}{d\Omega}d\Omega=\frac{1}{2N_t\phi}2\pi\int_0^\pi\frac{N(\theta)}{\Delta\Omega}\sin\theta d\theta$$
$$=\frac{\pi}{N_t\phi}(2A+\tfrac{4}{3}B+\tfrac{16}{15}C)\,. \tag{3}$$

Using a 2π geometry we have

$$\sigma_e=\frac{N}{N_t\phi}\,, \tag{4}$$

where N is the total number of fission events registered for 2π sr.

The term $N_t\phi$ appearing in Eqs. (1), (3), and (4) is given by

$$N_t\phi=\frac{N_0}{Aq_e}(XQ)\,,$$

where N_0 is Avogadro's number, A is the target mass number, q_e is the electron charge, X is the target thickness (in $\mu g/cm^2$), and Q is the integrated beam current (in μC).

From the virtual-photon formalism, the electrofission cross section, as a function of incident electron energy E_0, is given by

$$\sigma_e(E_0)=\sum_{\lambda L}\int_0^{E_0}\sigma^{\lambda L}(E)N^{\lambda L}(E,E_0)E^{-1}dE\,, \tag{5}$$

where λ identifies the electric or magnetic character of the transition and L its multipolarity, $N^{\lambda L}$ is the virtual-photon spectrum calculated in DWBA,[8] E is the real or virtual photon energy, and the photofission cross section σ is given by

$$\sigma(E)=\sum_{\lambda L}\sigma^{\lambda L}(E)\,, \tag{6}$$

where the $\sigma^{\lambda L}$ represent the partial cross sections for the transitions λL, both isoscalar and isovector, namely

$$\sigma^{\lambda L}(E)=\sigma^{\lambda L,s}(E)+\sigma^{\lambda L,v}(E)\,. \tag{7}$$

We next select the principal multipolar components λL present in the photofission process to be $E1$ and $E2$. Other multipolarities that possibly play a role are (a) $E0$, (b) $E3$, and (c) $M1$:

(a) Many theoretical calculations have predicted the existence of a giant $E0$ resonance, and some evidence for its observation has been reported recently.[23,24] The isovector mode has been predicted to be located at $\sim 178A^{-1/3}$ MeV, or at ~29 MeV for ^{236}U, and the isoscalar mode nearly to coincide with the isoscalar GQR, at $\sim 58A^{-1/3}$ MeV (Ref. 25); however, the available experimental evidence suggest its position to be much closer to the GDR ($\sim 78A^{-1/3}$ MeV).[23,24] In any case, the total electron inelastic-scattering cross section is dominated by small momentum-transfer events (corresponding to small scattering angles), for which the longitudinal component is small with respect to the transverse one.[26] Thus, inclusive electrodisintegration measurements, like the one reported here, are almost equivalent to thin-target bremsstrahlung photodisintegration measurements, with the exception that for the latter all multipole orders contribute equally.

(b) There are experimental observations regarding the existence of an isoscalar giant $E3$ resonance located at $\sim 32A^{-1/3}$ MeV and an isovector one at $\sim 172A^{-1/3}$ MeV,[2,27] which therefore lie outside the energy range covered in the present work (5 to 27 MeV). Moreover, for incident electrons in our energy range, the momentum transfer imparted to the nucleus is far below that for which $E3$ transitions become important (relative to $E1$ or $E2$ transitions). For these reasons, an $E3$ component is not included in the present data analysis.

(c) Notwithstanding some considerable controversy concerning the detection of a giant $M1$ resonance, the data to date suggest the probable occurrence of at least some $M1$ strength at ~40 $A^{-1/3}$ MeV,[3,4] and thus near the fission barrier for ^{236}U. Therefore, there is no argument which supports the exclusion of $M1$ strength *a priori* from the present study, except that there is no clear-cut experimental evidence supporting a concentration of $M1$ strength in heavy nuclei sufficiently strong to classify it as a giant resonance.

Then, for λL limited to $E1$, $E2$, and $M1$, one can eliminate σ^{E1} from Eqs. (5) and (6), groups terms, and apply certain small approximations[5] to obtain the cross-section difference

$$\Delta\sigma_e(E_0)\equiv\sigma_e(E_0)-\sigma_e^*(E_0)$$
$$=\sigma_e(E_0)-\int_0^{E_0}\sigma(E)N^{E1}(E,E_0)E^{-1}dE$$
$$=\int_0^{E_0}\sigma^{\mathrm{Add}}(E)[N^{E2}(E,E_0)-N^{E1}(E,E_0)]E^{-1}dE\,, \tag{8}$$

where σ_e^* is the $E1$ cross section, σ_e the total electrofission cross section, and

$$\sigma^{\mathrm{Add}}(E)=\sigma^{E2}(E)+F(E)\sigma^{M1}(E)\,, \tag{9}$$

where $\langle F(E)\rangle=\langle N^{M1}/N^{E2}\rangle$. The ratio $N^{M1}(E,E_0)/N^{E2}(E,E_0)$ in the region of excitation energy E near 6 or 7 MeV is almost independent of E_0; also, for E ranging from 5 to $\lesssim 7$ MeV the mean value for

$\langle N^{M1}/N^{E2}\rangle$ is equal to 3.1 with a dispersion of 0.2.[8] The cross section σ^{Add}, which is the solution of the integral equation (8), represents the contributions of the additional multipoles, i.e., those other than $E1$.

The main results of this work are obtained from a combined analysis of the absolute electrofission cross section σ_e measured at this laboratory and the absolute Los Alamos–Livermore photofission cross section σ. In order to be sure that the two sets of data, measured at two different laboratories, do not contain serious systematic errors working in opposite directions, which would result in a $\Delta\sigma_e$ with no physical meaning, we have obtained the bremsstrahlung-induced fission cross section σ_B by measuring the total number N_F of fission events at 2π sr, as described in Sec. II. Then the relation $\sigma_B = N_F/N_t\phi$ contains the same factor $N_t\phi$ that was used for the determination of σ_e. We have compared these values for σ_B, for $E_0 = 9$, 11, 13, 15, 17, and 19 MeV, with

$$\sigma_B(E_0) = \int_0^{E_0} \sigma(E) N_B(E, E_0) dE \qquad (10)$$

obtained from the numerical integration of $\sigma(E)$ in the bremsstrahlung-spectrum kernel N_B.

The kernel N_B in Eq. (10) is the thin-target bremsstrahlung spectrum,[28] corrected for the finite thickness of the radiator.[29] This correction consists of (a) dividing the radiator thickness t into n slices $t_n = t/n$ ($n \gtrsim 10$); (b) calculating $N_B(t_n)$ for each slice, taking into account the electron energy degradation in all the preceding slices; and (c) evaluating the integral of Eq. (10) in a multiple-step process for each $N_B(t_n)$. These calculations of $N_B(t_n)$ and $\int_0^{E_0} \sigma(E) N_B(E, E_0) dE$ are achieved with the use of the routine SABRE 2.[29] The combined uncertainty in the bremsstrahlung intensity and in these correction procedures does not exceed 10%.

The six values for the ratio of the experimental value for σ_B to that from Eq. (10) had a mean of 1.04 with a dispersion of less than 5%. This means that the quantity $\Delta\sigma_e$ cannot be attributed to fortuitous systematic errors, such as, for example, an overestimate of σ_e an underestimate of σ. It also means that the total absolute systematic uncertainties of both the São Paulo and Los Alamos–Livermore photofission measurements are less than 10%, and probably considerably less (unless they both are in the same direction, which would not appreciably affect the conclusions of this paper). An appreciable uncertainty of the $E1$ virtual-photon spectrum also can be ruled out, for the same reason.

Certain important points should be emphasized here:

(a) The presence or absence of contributions from multipoles other than $E1$ is determined only by the electrofission cross-section difference $\Delta\sigma_e$; that is, if $\Delta\sigma_e = 0$ the process is pure $E1$.

(b) The hypothesis of an $M1$ component in σ^{Add} is initially only a formal procedure; i.e., its effective presence (or absence) will be determined below, based upon the analysis of the fission-fragment angular distributions.

(c) The sensitivity of this method to detect the presence of an $M1$ component is embodied in the factor $F(E)$ of Eq. (9). It can be seen from the virtual-photon spectra shown in Fig. 1 that at energies near the end-point energy (9.5 MeV) the $M1$ spectrum is much more intense than the $E2$ spectrum; thus, even a small $M1$ component will produce a large electrofission yield in the low-energy region [since $F(E)$ is large there; see above].

(d) The bremsstrahlung-induced photofission cross section σ_B was measured only for cross-check purposes (as explained above) and is not used in the determination of the photofission components different from $E1$ in σ^{Add}.

IV. RESULTS AND DISCUSSION

A. Electrofission cross sections

The experimental results for the electrofission cross section σ_e are the data points shown in Fig. 2. Note that for all but the two lowest-energy points, the error flags are smaller than the plotted symbols. The error flags contain the propagation of both count-rate statistics (~1%) and systematic uncertainties (in the target thickness, mica-detector areas, and reaction-chamber radius); no un-

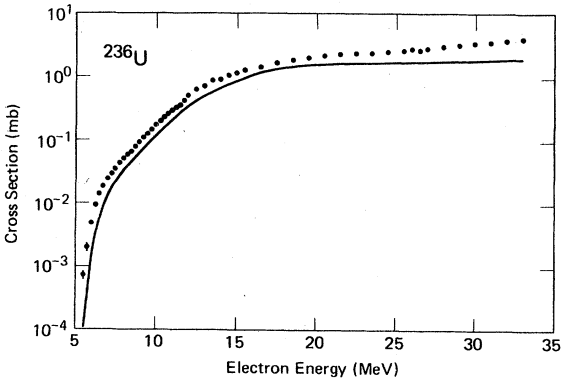

FIG. 2. Measured electrofission cross section σ_e for ^{236}U (data points). Except for the two lowest-energy points, the statistical uncertainties are smaller than the plotted symbols. The solid curve represents the cross section σ_e^* which would result from the $E1$ component only, obtained by integrating the photofission cross section $\sigma(E)$ of Ref. 18 with the $E1$ virtual-photon spectrum. The uncertainty here is of the order of the thickness of the line.

certainty has been included for the beam-monitoring device (see Sec. II). The solid curve in Fig. 2 represents the $E1$ cross section σ_e^* [Eq. (5)] which was calculated from the values for $\sigma(E)$ from Ref. 18 up to 18.3 MeV. Because of the lack of experimental data for the photofission of ^{236}U above this energy, the higher-energy values of σ_e^* were obtained by extrapolating the high-energy tail of $\sigma(E)$; it should be noted, however, that the high-energy behavior of σ_e^* is for all practical purposes insensitive to $\sigma(E)$—it does not vary appreciably even if we assume $\sigma(E)$ to be equal to zero above 20 MeV.

The differences $\Delta\sigma_e$ [Eq. (8)] between the electrofission cross section and the solid curve of Fig. 2 are shown in Fig. 3. The absolute uncertainty in the Los Alamos–Livermore cross section is less than 7%.[18] We included a 7% uncertainty in σ_e^* below 7 MeV and 5% above that energy in the error flags of Fig. 3, along with the uncertainties in σ_e listed above. In order to test whether the differences $\Delta\sigma_e = \sigma_e - \sigma_e^*$ can be attributed to an erroneous experimental procedure rather than to the presence of transition strength of multipolarity other than $E1$, we plot the ratio σ_e^*/σ_e as a function of E_0 in Fig. 4. First, it can be seen that this ratio is about 0.7 through most of the energy range (above ~8 MeV), indicating that such an error would have to reach 30%, which is unlikely. Moreover, the fact that σ_e^*/σ_e varies strongly below 8 MeV (from 0.1 to 0.7) proves the existence of a strongly varying σ^{Add} [Eqs. (8) and (9)] at these low energies.

Figure 5 shows σ^{Add} obtained by solving the integral equation (8), using the least-structure unfolding technique of Cook.[30] This unfolding technique is characterized by the smoothing out of any

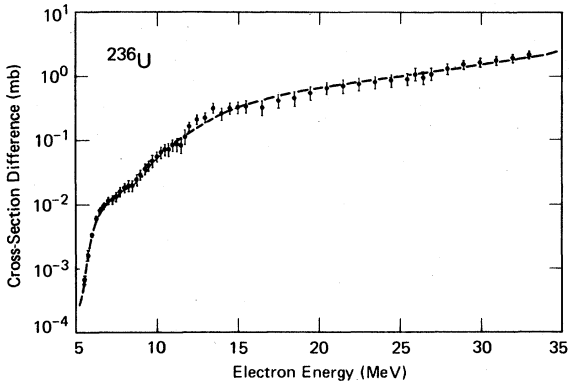

FIG. 3. Electrofission cross-section differences $\Delta\sigma_e$ between the data and the curve of Fig. 2 (data points). The dashed curve is the foldback of σ^{Add} in Eq. (8); i.e., insofar as the true representation of σ^{Add} is given by the curve of Fig. 5, then the cross-section differences plotted here should lie upon the dashed curve.

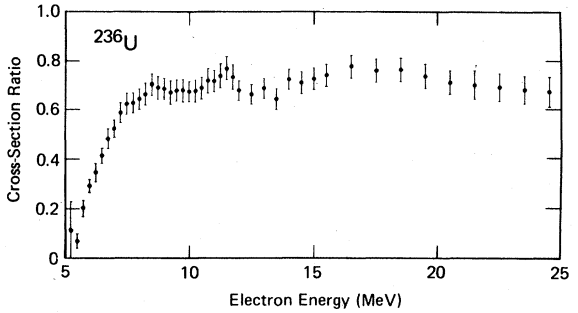

FIG. 4. The ratio of the $E1$ electrofission cross section and the total electrofission cross section for ^{236}U.

structure not compatible with the experimental errors (as long as it is not pushed too far in the attempt to delineate fine structure). This technique was not used above 23 MeV, because the experimental errors in $\Delta\sigma_e$ above that energy (see Fig. 3) are too large to yield an unambiguous and stable solution of Eq. (8) there. As will be seen below, however, it still is possible to establish both upper and lower limits on the strength of an (isovector) $E2$ resonance between about 23 and 30 MeV. The uncertainty in σ^{Add} (represented by the shaded band in Fig. 5) includes the uncertainties both in $\Delta\sigma_e$ and in the unfolding procedure. Until now there has been no precise test for the $E2$ virtual-photon spectrum; however, an upper limit of ~20% has been established as the maximum uncertainty.[10] The propagation of that ±20% in N^{E2} changes the fractional error in the strength $[\int \sigma^{\mathrm{Add}}(E)E^{-2}dE$, as discussed in Sec. IV C] to a value about twice as large.

B. Separation and delineation of the $E2$ and $M1$ components

From the previous discussion (Sec. III), we conclude that the cross section σ^{Add} (Fig. 5)

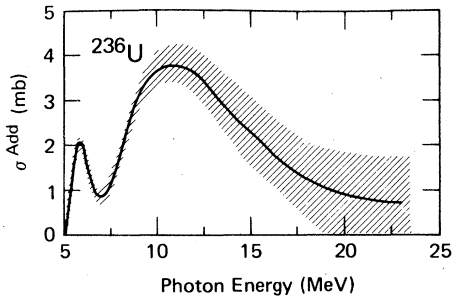

FIG. 5. "Additional" (of multipolarity other than $E1$) cross section $\sigma^{\mathrm{Add}}(E)$ for ^{236}U obtained by solving the integral equation (8) using the least-structure unfolding procedure of Ref. 30. Both systematic and statistical uncertainties are included in the error band.

represents either mainly $E2$ transitions or else a mixture of $E2$ strength plus some $M1$ strength, the latter amplified by the factor $F(E)$ [Eq. (9)]. The sharp peak in σ^{Add} at 5.8 MeV, corresponding to $\sim 40A^{-1/3}$ MeV, gives rise to a reasonable suspicion that it could result from a non-negligible $M1$ contribution. However, in order to test first whether, despite the strong smoothing inherent in the unfolding procedure, this peak could have arisen from an unknown experimental uncertainty in the determination of $\Delta\sigma_e$, we display in Fig. 6 a linear plot of $\Delta\sigma_e$ in the energy range from 5 to 7 MeV. [The point with no error bar at 5.25 MeV was obtained by assuming that $\sigma(E)$ falls exponentially below this energy (sub-barrier photofission).] It can be seen that there is a clear inflexion near 6 MeV that gives rise to the peak in σ^{Add}; in order to remove this inflexion from the data it would be necessary that (a) the values of $\Delta\sigma_e$ between 5 and 6 MeV be overestimated by almost 100%, and (b) the photofission cross section $\sigma(E)$ fall abruptly to zero at 5.3 MeV so that $\Delta\sigma_e \simeq 0$ for $E_0 = 5.3$ MeV. The first of these conditions is surely not reasonable, and the second is simply not true, as can be seen from the photofission cross-section data of Lindgren *et al.*[20] for ^{236}U between 5 and 7 MeV, which complement the Los Alamos–Livermore data[18] below the fission barrier and which were used in the present analysis. The structure found at 5.8 MeV could result, at least in part, from penetrability through the fission barrier; however, the analysis of the angular distributions (see below) can tell us how much of the strength concentrated in that structure results from transitions other than $E2$ ($M1$, in the present situation).

The angular distributions of electrofission fragments are given by the differential cross section

$$\frac{d\sigma_e(E_0)}{d\Omega} = A(E_0) + B(E_0)\sin^2\theta + C(E_0)\sin^2 2\theta \quad (11)$$

for $L = 1, 2$, where the coefficients A, B, and C are in units of mb/sr. For $L = 0$, the angular distribution is isotropic. It is customary to define the angular-distribution function $W(\theta)$ by

$$W(\theta) = a + b\sin^2\theta + c\sin^2 2\theta, \quad (12)$$

where the normalized and dimensionless coefficients a, b, and c are obtained from the A, B, and C of Eq. (11) by dividing them by $(2A + \frac{4}{3}B + \frac{16}{15}C)$; this latter quantity multiplied by 2π is the total electrofission cross section [Eq. (3)], so that the quantity $(2a + \frac{4}{3}b + \frac{16}{15}c)$ is normalized to unity.

Figure 7 shows the electrofission-fragment

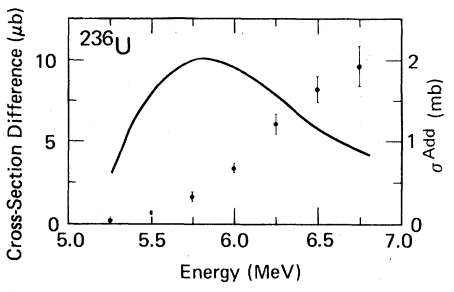

FIG. 6. Linear plot of the cross-section difference $\Delta\sigma_e$ (data points, scale on left), along with $\sigma^{\mathrm{Add}}(E)$ over the same low-energy range (solid curve, scale on right) for ^{236}U.

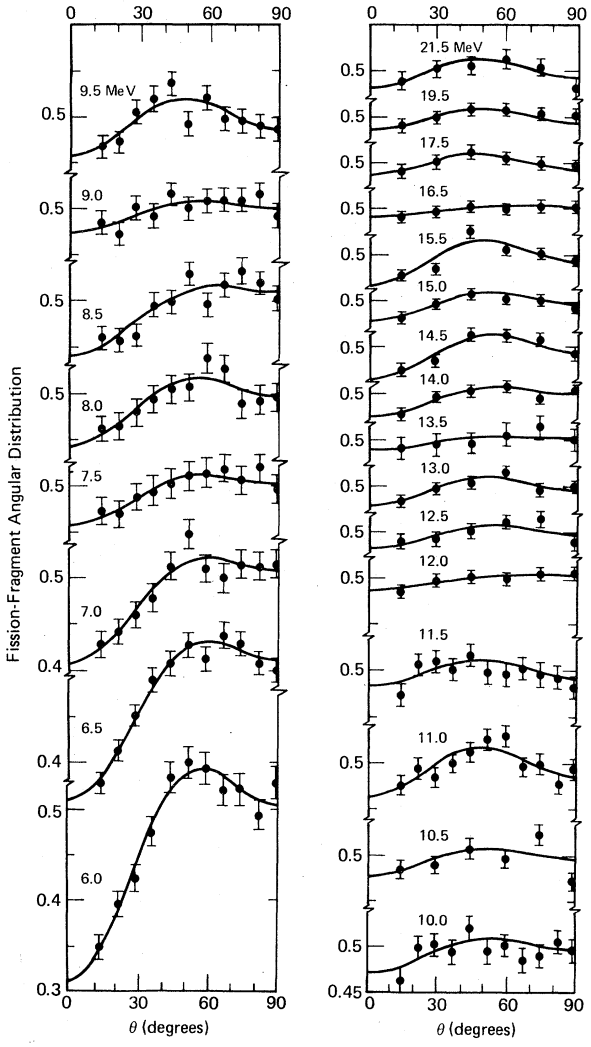

FIG. 7. Electrofission-fragment angular distributions for ^{236}U for incident electrons having energies from 6.0 to 21.5 MeV. The curves are least-square fits of the function $W(\theta)$ [Eq. (12)] to the experimental points. Both systematic and statistical uncertainties are included in the error flags, and were used in the fitting procedure. The redundant data points at 97.5° are not shown.

angular distributions $W(\theta)$ for ^{236}U for values of E_0 from 6.0 to 21.5 MeV. No angular-distribution data were obtained below 6.0 MeV; above 21.5 MeV the angular distributions were essentially isotropic, and hence are not presented here. The solid curves were obtained as least-squares fits of $W(\theta)$ [Eq. (12)] to the experimental points. It should be noted that systematic as well as statistical uncertainties have been included in the error flags on the points and were used in the fitting procedure. The systematic enhancement found in $W(\theta)$ near 45° reveals the presence of a major $E2$ component (at least up to ~11 MeV).

Assuming that near 6 MeV (in the fission-barrier region) all the $E2$ fission reactions proceed through the $K=0$ channel (K is the projection of the total angular momentum along the nuclear symmetry axis), we have[10,21] for the coefficient of $\sin^2 2\theta$ in Eq. (11)

$$C(E_0)=\frac{15}{32\pi}\int_0^{E_0}\sigma^{E2}(E)[N^{E2,1}(E,E_0)-\tfrac{3}{2}N^{E2,0}(E,E_0)-\tfrac{1}{4}N^{E2,2}(E,E_0)]\,E^{-1}dE, \tag{13}$$

where the $N^{E2,M}$ are the virtual-photon spectra for each magnetic substate M. The absolute values for $C(E_0)$ obtained from least-squares fit of Eq. (13) to the angular-distribution data are shown as the data points in Fig. 8. The dashed curve shown in Fig. 8 is obtained from Eq. (13) for the case $\sigma^{Add}=\sigma^{E2}$, i.e., assuming no $M1$ component; a large discrepancy between it and the data is observed. However, by assuming the existence of a small $M1$ component represented by a Breit-Wigner shape at 5.8 MeV having a width of 1 MeV and a peak cross section of 0.4 mb, subtracting it from σ^{Add} [taking into account the amplication factor $F(E)$], and again integrating Eq. (13), we obtain the solid curve shown in Fig. 8. This curve agrees with the data up to ~6.5 MeV;

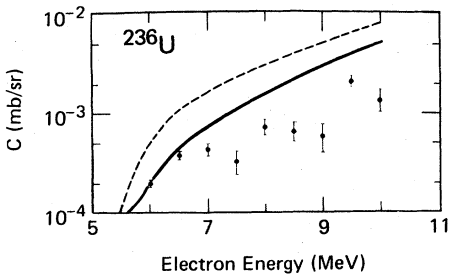

FIG. 8. Absolute values for the coefficient of the $\sin^2 2\theta$ term in the electrofission differential cross section $C(E_0)$ [Eq. (11)], obtained from the measured angular distributions for ^{236}U (data points). The solid curve represents this coefficient as computed, using Eq. (13), from σ^{Add} after $M1$ subtraction; the dashed curve assumes there to be no $M1$ component in σ^{Add}.

at this energy the opening of the $K=1$ fission channel acts to reduce $C(E_0)$,[21] so that the fact that the data points shown in Fig. 8 fall below the solid curve above this energy is expected. The results of this decomposition of σ^{Add} into its $E2$ and $M1$ components are shown in Fig. 9. From Eq. (9) and the $\sigma^{M1}(E)$ obtained above we determine $\sigma^{E2}(E)$ to be equal to $\sigma^{Add}(E)-\langle F(E)\rangle\sigma^{M1}(E)$. Although the uncertainty in the strength of the $M1$ component obtained from this analysis is of the order of 20%, its location is well fixed by the pronounced peak in σ^{Add} at 5.8 MeV.

A stringent test of our technique and result is obtained from a comparison with the photofission angular distributions. Figure 10 shows (as the data points) the values for σ^{E2} obtained from

$$\sigma^{E2}(E)=\frac{8c(E)/15}{a(E)+2b(E)/3+8c(E)/15}\,\sigma(E) \tag{14}$$

for the $K=0$ channel, where the values for the coefficients a, b, and c are taken from the photofission angular-distribution data of Ref. 20 and $\sigma(E)$ from Ref. 18 as before. This procedure gives σ^{E2} normalized to the Los Alamos–Livermore cross section.[18] The lower solid curve, which agrees very well indeed with the data points, is the result for $\sigma^{E2}(E)$ of the above analysis, while the upper solid curve corresponds to the case $\sigma^{E2}=\sigma^{Add}$. This comparison shows that the structure observed in σ^{Add} at 5.8 MeV is incompatible with a pure $E2$ hypothesis, confirming the electrofission angular-distribution results (Fig. 8), whether or not its assignment is $M1$.

Owing to the controversial nature of the results reported to date in the literature related to the detection of $M1$ strength in heavy nuclei, we comment here on certain other possible sources of error regarding the present $M1$ assignment:

(a) The possibility of an appreciable difference in the energy scales for the two sets of data (σ_θ and σ_θ^*) used to determine $\Delta\sigma_\theta$ can be discarded because our bremsstrahlung cross check is very sensitive to such a calibration difference, par-

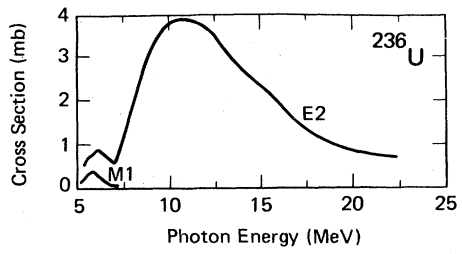

FIG. 9. Partial photofission cross sections $\sigma^{E2}(E)$ and $\sigma^{M1}(E)$ for ^{236}U, obtained from the decomposition of $\sigma^{Add}(E)$ (Fig. 5), as described in the text.

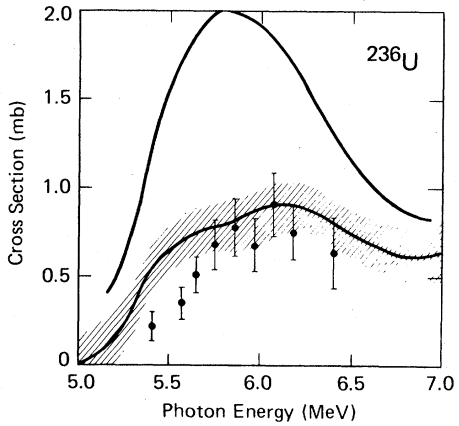

FIG. 10. $E2$ photofission cross section $\sigma^{E2}(E)$ for ^{236}U, obtained, using Eq. (14), from the total photofission cross-section data of Ref. 18 and the photofission angular-distribution data of Ref. 20 (data points). The lower solid curve with the error band is $\sigma^{E2}(E)$ from Fig. 9; the upper solid curve is $\sigma^{\mathrm{Add}}(E)$ from Fig. 5.

ticularly below 16 MeV, where the slopes of the integral $\int_0^{E_0}\sigma(E)N_B(E,E_0)dE$ [Eq. (10)] and of the cross section $\sigma_B(E_0)$ are accentuated. Changes in energy as small as ~0.3 MeV would have been noticed, whereas the electron-beam energy resolution is 1% (much smaller than 0.3 MeV).

(b) Since the $M1$ strength reported here is concentrated near the neutron-emission threshold, it is natural to suspect that the onset of the neutron-emission channel would bleed off much of the strength from the fission channel and thus give rise to the observed peak at 5.8 MeV. However, the photoneutron threshold for ^{236}U is greater than 6.5 MeV, and $\sigma^{\mathrm{Add}}(E)$ already is decreasing at least 0.5 MeV below that energy; therefore, the onset of the neutron-emission channel plays no important role in our $M1$ assignment.

(c) Among the parameters obtained for the $M1$ component, the strength is the one that depends most strongly upon the angular-distribution coefficient $C(E_0)$. The formalism that results in Eq. (13) assumes that K (the angular-momentum projection) is a good quantum number, and although there is no evidence to date that this is not true, we cannot evaluate the exact extent to which a breakdown of this assumption would affect the magnitude of the assigned $M1$ strength. The inclusion of K mixing in the fission process mainly involving an admixture of $K=1$ strength into the predominantly $K=0$ cross section would decrease the values of $C(E_0)$ which have been obtained from Eq. (13), and consequently, if this were the case, the $M1$ strength would have been overestimated here. On the other hand, it would appear from the change in slope of $C(E_0)$ near 6.5 MeV for ^{236}U (Fig. 8), as well as for ^{238}U (Ref. 21), that a well-defined threshold for the opening of the $K=1$ channel has been established, at least for these nuclei.

Finally, since for this case there is no discrimination against either isoscalar or isovector modes, we have, from Eq. (7), that

$$\sigma^{E2}(E)=\sigma^{E2,s}(E)+\sigma^{E2,v}(E). \tag{15}$$

For ^{236}U the separation between the peaks corresponding to $\sigma^{E2,s}$ and $\sigma^{E2,v}$ is ~13 MeV, which leads us to conclude that the GQR obtained here (Fig. 9) is predominantly isoscalar. The question of isovector $E2$ strength above ~20 MeV will be discussed below.

C. Comments on the GQR parameters

The position of the resonance peak ($\sim 67A^{-1/3}$ MeV), given in Table I, agrees reasonably well with the experimental systematics for other heavy nuclei.[2,3]

The width (~8 MeV; see Fig. 9) is considerably larger than the experimental systematics for other heavy nuclei. We note here that these large widths are not artifacts of the unfolding procedure;[30] we found that reasonable changes in the smoothing parameter used in the unfolding procedure have very little effect on the widths of the structure obtained. On the other hand, our technique for the determination of σ^{E2} does not differentiate between first- and second-chance fission, and both are included in the $E2$ cross section of Fig. 9. In an attempt to subtract the second-chance $E2$ photofission cross section σ_{nf}^{E2} from the total $E2$ photofission cross section $\sigma_F^{E2}=\sigma_f^{E2}+\sigma_{nf}^{E2}$, we have assumed, as in Ref. 17, that the ratio

TABLE I. Parameters for first-chance fission decay of the GQR.

Nucleus	Peak energy (MeV)	FWHM (MeV)	% EWSR 1 Unit[a]	% EWSR 1.3 Units[b]	Reference
^{236}U	10.8±0.4	~6	72±10	≃55	Present work
^{238}U	9.9±0.4	~5	≳55	≳42	5, 17

[a] Assumes that the total $E2$-photoabsorption strength exhausts one isoscalar EWSR unit.
[b] Assumes that 1.3 EWSR units (130% of the isoscalar $E2$ sum rule) are exhausted (see text).

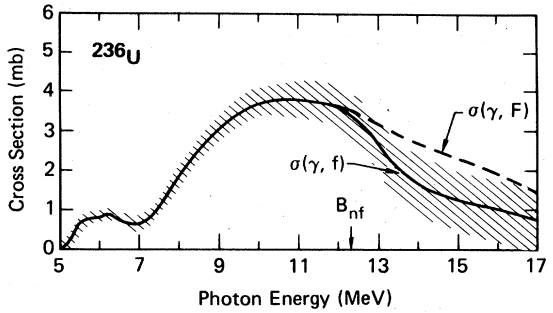

FIG. 11. First-chance $E2$ photofission cross section $\sigma^{E2}(\gamma,f)$ (solid curve), obtained from the total $E2$ photofission cross-section $\sigma^{E2}(\gamma,F)$ (solid curve below the second-chance fission barrier B_{nf}= 12.3 MeV, dashed curve above B_{nf}) as described in the text. Both systematic and statistical uncertainties are included in the error band.

$\sigma_f^{E2}/\sigma_F^{E2}$ for $E2$ transitions is the same as that obtained experimentally[18] for $E1$ transitions. Figure 11 shows both the first- and second-chance $E2$ photofission cross sections from the decomposition of the total cross section (σ_F^{E2}; Fig. 9), and all the parameters are given in Table I, along with those previously obtained for ^{238}U (Refs. 5 and 17). The width, equal to ~6 MeV, is still large, but it should be noted that the ^{236}U nucleus, like ^{238}U, is statically deformed.[18] The splitting of the GDR for statically deformed nuclei has been studied extensively and is at present well established.[1,18,31-34] However, it is still an open question as to whether and to what extent the GQR for deformed nuclei also are split or broadened or both. Predictions regarding the splitting of both isoscalar and isovector giant $E2$ resonances have been made,[35,36] and their broadening has been treated in terms of a quadrupole-quadrupole nucleon-nucleon effective interaction.[37] Broadenings of ~1 MeV between ^{144}Sm and ^{154}Sm and ~2 MeV between ^{142}Nd and ^{150}Nd have been observed in measurements of the GQR by means of the (d,d') and (e,e') reactions, respectively.[37,38] Therefore, the possibility of a substantial broadening of the GQR for ^{236}U cannot be discarded.

The strength of (72 ± 10)% of one EWSR (energy-weighted sum rule) unit, after subtraction of the second-chance fission cross section, shows the likely dominance of the fission channel in the decay of the GQR for ^{236}U. Assuming an uncertainty of ± 20% in the $E2$ virtual-photon spectrum, we obtain an uncertainty of ~± 30% in the strength, that is, (72 ± 22)% of one EWSR unit, and even the lower limit for this strength (72% − 22% = 50%) is still larger than the GDR fission-decay strength (34%).[18]

It has been found, moreover, that for ^{236}U the fission probability P_f in the energy range from 6 to 12 MeV is nearly constant and lies between 0.3 and 0.4 for photofission[18] (which is dominated by $L=1$ excitation), but lies somewhat higher, between 0.5 and 0.8, for excitation energies from 6 to 7 MeV, for the (t,pf) reaction[39,40] (for which several L values are important). In a recent study[17] we have shown again that the fission barrier heights B_f play a critical role in the determination of the fission probabilities; in particular, a change of only 0.5 MeV in the barrier heights causes an appreciable change in P_f (for the GQR fission near 10 MeV), namely, a sharp increase, from $P_f = 0.5$ to $P_f = 0.9$. This calculation was performed with a conventional statistical model using a Fermi-gas level density. In such a calculation, if a given nucleus has $B_f(J^\pi = 2^+) < B_f(J^\pi = 1^-)$, then $P_f(\text{GQR}) > P_f(\text{GDR})$. We refer the reader to Ref. 17 for a more complete discussion.

Finally, it should be noted that the calculation of the EWSR strength depends upon several assumptions, the most important of which is the value assumed for the nuclear radius parameter R_0. [We have taken R_0 to be 1.15 fm (see Ref. 18), from which the EWSR prediction for σ_{-2} (the second moment of the integrated cross section) is 0.329 mb MeV^{-1} for ^{236}U.] Moreover, there is no guarantee *a priori* that the total isoscalar $E2$ value for σ_{-2} does not exceed the EWSR prediction; it is well known,[1] for example, that the integrated GDR typically exceeds the Thomas-Reiche-Kuhn (TRK) sum-rule prediction by some 20% [and for ^{236}U, by 26% (Ref. 18)]. If, for instance, the nuclear radius parameter were underestimated by 10%, the new value for the total isoscalar $E2$ sum rule would increase by ~20%. Also, a recent measurement[41] of the GQR in ^{232}Th(α,α') found evidence supporting a strength of 130% of the EWSR. For illustrative purposes (only), we show in Table I how the results would look if the GQR were to exhaust 130% of the $E2$ isoscalar EWSR.

D. The $M1$ component

The strength of the $M1$ component in the fission channel for ^{236}U is very small (less than 2% of the $E2$ strength). However, it is worth emphasizing that its detection was made possible not only because of the greater intensity of the $M1$ virtual-photon spectrum than that of the $E2$ spectrum [by the factor $F(E)$], but also because it is more concentrated in energy than the $E2$ strength. Such a peak in the $M1$ strength could result from the $(1^+,1)$ level of the transition nucleus (the saddle point), as in ^{238}U, located around 6 MeV, and not from a resonance of the $M1$ photoabsorption process. The relatively broad width of 1 MeV (compared to a narrow level) could owe its origin partly to the smoothing technique employed in the unfolding procedure and partly to the finite energy

resolution associated with the determination of $\Delta\sigma$ (from the 0.25-MeV steps).

E. Limits on the isovector $E2$ strength

It has been predicted, in Refs. 35, 42, and elsewhere, that the isovector GQR strength greatly exceeds the isoscalar strength. Yet, the experimental results for both ^{236}U and ^{238}U (Ref. 5) indicate that very little isovector $E2$ strength appears in the fission channel, even though a substantial isovector GQR is seen in the neutron-emission channel.[1,43]

The unfolding of $\sigma^{\mathrm{Add}}(E)$ from the cross-section differences $\Delta\sigma_e$ was carried out above only up to ~23 MeV, owing to the fact that large uncertainties are associated with the high-energy tail of $\sigma^{\mathrm{Add}}(E)$ (see Fig. 5), where the isovector $E2$ strength is expected to lie. Since, however, $\Delta\sigma_e$ is an integrated cross section, it will be sensitive to the presence of an appreciable isovector $E2$ component only at higher energies (>30 MeV). In order to establish limits on the isovector $E2$ strength, we carried out some simulations. Initially we separated the quantities $\sigma^{E2,s}$ and $\sigma^{E2,v}$ of Eq. (15) explicitly in Eq. (8); i.e.,

$$\Delta\sigma_e = \int_0^{E_0} [\sigma^{E2,s}(E) + F(E)\sigma^{M1}(E)] \times [N^{E2}(E,E_0) - N^{E1}(E,E_0)]\,E^{-1}dE + \int_0^{E_0} \sigma^{E2,v}(E)[N^{E2}(E,E_0) - N^{E1}(E,E_0)]\,E^{-1}dE . \quad (16)$$

The simulations consisted of assuming the presence of an isovector $E2$ component $\sigma^{E2,v}$ near 22 MeV having a width of about 7 MeV, folding back Eq. (16), and calculating the values for χ^2 between the experimental $\Delta\sigma_e$ and the $\Delta\sigma_e$ obtained by numerical integration of Eq. (16) over the energy range from 23 to 33 MeV (the last experimental data point). Values for χ^2 of ~1.0 were obtained for isovector $E2$ strengths from a lower limit of zero to an upper limit of ~10% of the corresponding EWSR. Thus, the electrofission yields above 23 MeV are compatible with an isovector $E2$ component that exhausts no more than 10% of the EWSR in the fission channel for ^{236}U.

One would expect a suppression of the fission component for any isovector excitation, since the classical description of such an excitation consists of a vibration of the neutrons against the protons in the nucleus (like the hydrodynamic model of the GDR), and this motion would have to get damped into the compound nucleus before fission could take place. One also might expect that at the higher excitation energy of the isovector GQR there would be a larger direct-reaction component, which also would favor neutron emission over fission. But it is somewhat surprising that even both of these effects combined could suppress completely the fission decay of the isovector GQR. Nevertheless, this apparent selectivity of the fission decay channel with respect to the isoscalar or isovector nature of the mode of excitation of the GQR might very well prove to be a valuable tool for studying collective excitations in nuclei.

V. CONCLUSIONS

The characteristics and parameters of the isoscalar GQR and, more tentatively, a small $M1$ component for ^{236}U have been delineated in this work, with the results given in Fig. 11 and Table I, and limits have been set on the isovector GQR component in the fission channel. These results depend upon the precise knowledge of both the electrofission and photofission cross sections and of the virtual-photon spectra in order that the extraction of the $E2$ and $M1$ components of the photofission cross section be unambiguous. This being the case, in our judgment, we believe that the present results add significantly to our knowledge of the excitation and decay mechanisms of the new giant resonances. Clearly, further studies, for the actinide nuclei and for other nuclei as well, should be pursued in order to expand our knowledge of the systematics of these important collective features of the nuclear spectrum.

ACKNOWLEDGMENTS

We are pleased to acknowledge the able assistance of A. Vannucci, R. Hermann, and M. F. B. Monteiro in preparing the mica foils and reducing the data. We benefited as well from valuable discussions with Dr. M. G. Mustafa, Dr. M. S. Weiss, Prof. A. K. Kerman, and Dr. A. C. Shotter. Finally, thanks are due to Dr. J. G. Povelites for preparing the uranium target foils. This work was supported in part by the Fundação de Amparo à Pesquisa do Estado de São Paulo and the Conselho Nacional de Desenvolvimento Científico e Tecnológico.

*Present address: High Energy Physics Laboratory, Stanford University, Stanford, California 94305.
†Permanent address: Lawrence Livermore Laboratory, University of California, Livermore, California 94550.

[1]B. L. Berman and S. C. Fultz, Rev. Mod. Phys. 47, 713 (1975).
[2]F. E. Bertrand, Annu. Rev. Nucl. Sci. 26, 457 (1976).
[3]S. S. Hanna, *International School on Electro and Photonuclear Reactions*, edited by S. Costa and C. Schaerf [Lecture Notes in Physics Vol. 61 (Springer, New York, 1977)].
[4]L. W. Fagg, Rev. Mod. Phys. 47, 683 (1975).
[5]J. D. T. Arruda Neto, S. B. Herdade, B. S. Bhandari, and I. C. Nascimento, Phys. Rev. C 18, 863 (1978).
[6]J. D. T. Arruda Neto, B. L. Berman, S. B. Herdade, and I. C. Nascimento, Lett. Nuovo Cimento 26, 487 (1979).
[7]A. Bohr and B. R. Mottelson, *Nuclear Structure* (Benjamin, Reading, 1975), Vol. II.
[8]W. W. Gargaro and D. S. Onley, Phys. Rev. C 4, 1037 (1971).
[9]I. C. Nascimento, E. Wolynec, and D. S. Onley, Nucl. Phys. A246, 210 (1975).
[10]J. D. T. Arruda Neto, B. L. Berman, S. B. Herdade, and I. C. Nascimento, Phys. Rev. C (to be published).
[11]J. D. T. Arruda Neto, S. B. Herdade, B. S. Bhandari, and I. C. Nascimento, Phys. Rev. C 14, 1499 (1976).
[12]A. C. Shotter, D. Branford, J. C. McGeorge, and J. M. Reid, Nucl. Phys. A290, 55 (1977).
[13]U. Kneissl, G. Kuhl, K. H. Leister, and A. Weller, Nucl. Phys. A256, 11 (1976).
[14]M. B. Lewis and D. J. Horen, Phys. Rev. C 10, 1099 (1974).
[15]J. van der Plicht, M. N. Harakeh, A. van der Woude, P. David, and J. Debrus, Phys. Rev. Lett. 42, 1121 (1979).
[16]A. C. Shotter, C. K. Gelbke, T. C. Awes, B. B. Back, J. Mahoney, T. J. M. Symons, and D. K. Scott, Phys. Rev. Lett. 43, 569 (1979).
[17]J. D. T. Arruda Neto and B. L. Berman, Nucl. Phys. (to be published).
[18]J. T. Caldwell, E. J. Dowdy, B. L. Berman, R. A. Alvarez, and P. Meyer, Phys. Rev. C 21, 1215 (1980).
[19]M. V. Yester, R. A. Anderl, and R. C. Morrison, Nucl. Phys. A206, 593 (1973).
[20]L. J. Lindgren, A. Alm, and A. Sandell, Nucl. Phys. A298, 43 (1978).
[21]J. D. T. Arruda Neto, S. B. Herdade, and I. C. Nascimento, Nucl. Phys. A334, 297 (1980).
[22]W. C. Barber, Phys. Rev. 111, 1642 (1958).
[23]S. Fukuda and Y. Torizuka, Phys. Lett. 62B, 146 (1976).
[24]D. H. Youngblood, C. M. Rozsa, J. M. Moss, D. R. Brown, and J. D. Bronson, Phys. Rev. Lett. 39, 1188 (1977).
[25]T. Suzuki, Nucl. Phys. A217, 182 (1973).
[26]R. H. Dalitz and D. R. Yennie, Phys. Rev. 105, 1598 (1957).
[27]L. A. Malov, V. O. Nesterenko, and V. G. Soloviev, J. Phys. G 3, L219 (1977).
[28]L. I. Schiff, Phys. Rev. 83, 252 (1951).
[29]A. N. Fagundes, M. Sc. thesis, University of São Paulo, 1977 (unpublished).
[30]B. C. Cook, Nucl. Instrum. Methods 24, 256 (1963).
[31]B. L. Berman, M. A. Kelly, R. L. Bramblett, J. T. Caldwell, H. S. Davis, and S. C. Fultz, Phys. Rev. 185, 1576 (1969).
[32]P. Carlos, H. Beil, R. Bergère, A. Leprêtre, and A. Veyssière, Nucl. Phys. A172, 437 (1971).
[33]A. Veyssière, H. Beil, R. Bergère, P. Carlos, A. Leprêtre, and K. Kernbach, Nucl. Phys. A199, 45 (1973).
[34]P. Carlos, H. Beil, R. Bergère, A. Leprêtre, A. de Miniac, and A. Veyssière, Nucl. Phys. A225, 171 (1974).
[35]R. Ligensa and W. Greiner, Nucl. Phys. A92, 673 (1967).
[36]T. Suzuki and D. J. Rowe, Nucl. Phys. A289, 461 (1977).
[37]T. Kishimoto, J. M. Moss, D. H. Youngblood, J. D. Bronson, C. M. Rozsa, D. R. Brown, and A. D. Bacher, Phys. Rev. Lett. 35, 552 (1975).
[38]A. Schwierczinski, R. Frey, E. Spamer, H. Theissen, and Th. Walcher, Phys. Lett. 55B, 171 (1975).
[39]J. D. Cramer and H. C. Britt, Phys. Rev. C. 2, 2350 (1970).
[40]B. B. Back, O. Hansen, H. C. Britt, and J. D. Garrett, Phys. Rev. C 9, 1924 (1974).
[41]M. N. Harakeh, M. P. Morsch, K. van der Weg, A. van der Woude, and F. E. Bertrand, Phys. Rev. C 21, 768 (1980).
[42]M. A. Kiselev, L. A. Malov, V. O. Nesterenko, and V. G. Soloviev, Joint Institute for Nuclear Research (Dubna) Report No. E4-11121 (1978).
[43]B. L. Berman, D. D. Faul, R. A. Alvarez, P. Meyer, and D. L. Olson, Phys. Rev. C 19, 1205 (1979).